



UNIVERSITÀ
DEGLI STUDI
DI PADOVA

Università degli Studi di Padova

Padua Research Archive - Institutional Repository

Fe-rich ferropericlase and magnesiowüstite inclusions reflecting diamond formation rather than ambient mantle

Original Citation:

Availability:

This version is available at: 11577/3283786 since: 2020-01-09T14:24:32Z

Publisher:

Published version:

DOI: 10.1130/G45235.1

Terms of use:

Open Access

This article is made available under terms and conditions applicable to Open Access Guidelines, as described at <http://www.unipd.it/download/file/fid/55401> (Italian only)

(Article begins on next page)

1 This is a post-peer-review, pre-copyedit version of an article published in Geology. The
2 final authenticated version is available online at: <https://doi.org/10.1130/G45235.1>

3
4 **Fe-rich ferropericlase and magnesiowüstite inclusions**
5 **reflecting diamond formation rather than ambient mantle**

6 **Paolo Nimis¹, Fabrizio Nestola¹, Mariangela Schiazza^{1*}, Riccardo Reali², Giovanna**
7 **Agrosi³, Daniela Mele³, Giocchino Tempesta³, Daniel Howell^{1,4}, Mark T.**
8 **Hutchison⁵, and Richard Spiess¹**

9 *¹Dipartimento di Geoscienze, Università di Padova, via G. Gradenigo 6, 35131 Padova,*
10 *Italy*

11 *²Unité Matériaux et Transformations, Université Lille1, 59655 Villeneuve d'Ascq, France*

12 *³Dipartimento di Scienze della Terra e Geoambientali, Università degli Studi di Bari*
13 *Aldo Moro, Via Orabona 4, 70125 Bari, Italy*

14 *⁴Department of Earth Sciences, University of Bristol, Bristol, BS8 1RJ, UK*

15 *⁵Trigon GeoServices Ltd., Las Vegas, Nevada 89146, USA*

16 *Current address: Dipartimento di Scienze Psicologiche, della Salute e del Territorio
17 DiSPuTer, Università G. D'Annunzio di Chieti-Pescara, 66100 Chieti, Italy

18 **ABSTRACT**

19 At the core of many Earth-scale processes is the question of what the deep mantle
20 is made of. The only direct samples from such extreme depths are diamonds and their
21 inclusions. It is often assumed that these inclusions reflect ambient mantle or are
22 syngenetic with diamond, but these assumptions are rarely tested. We have studied
23 inclusion–host growth relationships in two potentially superdeep diamonds from Juina

24 (Brazil) containing nine inclusions of Fe-rich ($X_{\text{Fe}} \approx 0.33$ to ≥ 0.64) ferropericlasite–
25 magnesiowüstite (FM) by X-ray diffractometry, X-ray tomography,
26 cathodoluminescence, electron backscatter diffraction and electron microprobe analysis.
27 The inclusions share a common [112] zone axis with their diamonds and have their major
28 crystallographic axes within 3–8° of those of their hosts. This suggests a specific
29 crystallographic orientation relationship (COR), resulting from interfacial energy
30 minimization, disturbed by minor post-entrapment rotation around [112] due to plastic
31 deformation. The observed COR and the relationships between inclusions and diamond
32 growth zones imply that FM nucleated during the growth history of the diamond.
33 Therefore, these inclusions may not provide direct information on the ambient mantle
34 prior to diamond formation. Consequently, a ‘non-pyrolitic’ composition of the lower
35 mantle is not required to explain the occurrence of Fe-rich FM inclusions in diamonds.
36 By identifying examples of mineral inclusions which reflect the local environment of
37 diamond formation and not ambient mantle, we provide both a cautionary tale and a
38 means to test diamond/inclusion time relationships for proper application of inclusion
39 studies to whole-mantle questions.

40 INTRODUCTION

41 Diamonds found in kimberlites and lamproites are our deepest samples of Earth’s
42 interior. Most diamonds come from deep lithospheric roots beneath cratons, but some
43 rare diamonds are believed to have formed at sublithospheric levels, possibly as deep as
44 the core/mantle boundary (see reviews in Stachel et al., 2005; Harte, 2010; Kaminsky,
45 2012). Ferropericlasite–magnesiowüstite (Mg,Fe)O (hereafter FM) is the most common
46 mineral contained in diamonds of interpreted lower-mantle origin and its composition has

47 been recently used to estimate oxygen fugacity in the lower mantle (Otsuka et al., 2013;
48 Kaminsky et al., 2015). This is notwithstanding the fact that FM also participates in
49 mineral parageneses straddling the upper mantle/lower mantle boundary (Hutchison et
50 al., 2001), the relative abundance of FM inclusions is higher than predicted by
51 experiments on ‘pyrolite’ at lower-mantle conditions (48%–63% versus 16%–20%; e.g.,
52 Irifune, 1994; Fei and Bertka, 1999; Wood, 2000; Kaminsky, 2012), and their
53 composition is more variable and often more Fe-rich than expected for FM in the lower
54 mantle [$\text{Fe}/(\text{Mg} + \text{Fe})_{\text{mol}} = X_{\text{Fe}} = 0.10\text{--}0.64$ versus $0.10\text{--}0.27$; e.g., Kesson and Fitz
55 Gerald, 1992; Wood, 2000; Lee et al., 2004]. Fe-rich compositions characterize a
56 significant proportion (ca. 46.5%) of FM inclusions in Brazilian stones (Kaminsky,
57 2012).

58 Several hypotheses have been put forward to explain the existence of Fe-rich FM.
59 These hypotheses can be grouped into two categories: (i) the Fe-rich composition is
60 considered to reflect a ‘non-pyrolitic’ composition of the ambient lower mantle, samples
61 of which were captured by the growing diamonds (Harte et al., 1999; Kaminsky, 2012;
62 Ryabchikov and Kaminsky, 2013; Kaminsky and Lin, 2017); (ii) formation of Fe-rich
63 FM *and* diamond is ascribed to reactions involving carbonate melts or minerals in the
64 lower mantle (Liu, 2002; Litvin, 2014) or in the deep upper mantle and transition zone
65 (Thomson et al., 2016). This contrast of views is partly justified by the fact that the
66 traditional criterion used to identify syngenetic inclusions (i.e., a diamond-imposed
67 shape) has proven unreliable (Nestola et al., 2014). Therefore, there is still uncertainty as
68 to whether Fe-rich FM inclusions represent accidentally encapsulated portions of an
69 anomalous ambient mantle or a product of reactions occurring during the growth history

70 of diamond. As diamonds and their mineral inclusions are such important windows on
71 mantle composition and processes it is critical to test these conflicting hypotheses. This
72 may have profound implications on our interpretation of the mechanisms of formation of
73 sublithospheric diamonds and on the significance of petrological and geochemical data
74 extracted from their inclusions (e.g., Shirey et al., 2013; Thomson et al., 2014, 2016).

75 Here we investigate the growth relationships of nine Fe-rich ($X_{\text{Fe}} = 0.33$ to ≥ 0.64)
76 FM inclusions in two diamonds from the notable alluvial deposits of tributaries of the Rio
77 Aripuanã, Juina district, Brazil (e.g., Hutchison et al., 2004; see detailed provenance data
78 in the GSA Data Repository¹). We will show that our Fe-rich FM formed by direct
79 segregation from a fluid or melt or from fluid/melt-assisted dissolution-precipitation
80 during the growth history of their diamond hosts. Hence, the entrapped FM inclusions
81 should not be considered as representative samples of the ambient mantle in which the
82 diamond-forming processes took place.

83 **SAMPLE MATERIAL AND ANALYTICAL METHODS**

84 The diamonds studied in the present work (BZ270 and JUc4) appeared as
85 irregular, brown-colored stones, with maximum dimensions of 7 and 3 mm, respectively.
86 Sample preparation and analyses were conducted in such a way as to preserve as much of
87 the samples as possible for future investigations. The stones were polished on two
88 opposite sides to obtain small windows that allowed visual recognition of most of their
89 inclusions. The FM inclusions showed a faceted to subround shape, sometimes with
90 concave angles, and maximum dimensions of a few 10s to 500 μm (Fig. 1A,B). The
91 largest inclusions in diamond BZ270 exhibited stepped surfaces on some of the faces
92 (Fig. 1B). Decompression cracks were observed around most of the inclusions. Micro-

93 computed X-ray tomography (μ -CT) of diamond BZ270 showed the presence of
94 numerous additional inclusions, which have a size up to a few μm and are distributed
95 along a set of interconnected $\{111\}$ diamond planes (Fig. 1C and supplementary video in
96 the Data Repository).

97 Previous investigation by X-ray diffraction topography (XRDT) showed that both
98 samples are affected by plastic deformation (Agrosi et al., 2017). BZ270 is more strongly
99 deformed and consists of an aggregate of different 'grains', which are misoriented by at
100 least a few seconds of arc, whereas JUc4 appears to be a single grain. Micro Fourier-
101 transform infrared spectroscopy (μ FTIR) (Agrosi et al., 2017) showed that BZ270 was
102 predominantly Type IIa (i.e., nitrogen below detection of ~ 10 ppm; Fig. 2D). The μ FTIR
103 of a portion of JUc4 suggested the presence of a more N-rich core (270 ppm N, 100%
104 IaB, no platelets) and decreasing N content toward the rim (~ 40 ppm, 100% IaB, no
105 platelets) (Fig. 1E).

106 Both samples were studied by single-crystal X-ray diffraction (XRD) to determine
107 the approximate chemical compositions of the FM inclusions and their crystallographic
108 orientation relationships (CORs) with the diamonds. Diamond BZ270 was then further
109 polished to expose some of the large and small inclusions and investigated by
110 cathodoluminescence (CL) and electron backscatter diffraction (EBSD). Electron
111 microprobe analysis (EMPA) was performed on the exposed inclusions (Table DR1).
112 Additional details on analytical methods are given in the Data Repository¹.

113 **RESULTS**

114 The analyzed FM inclusions have their major crystallographic axes within $3\text{--}8^\circ$ of
115 those of the host diamonds (Fig. 2, Table DR2). Despite this minor misorientation, the

116 angular mismatch between the [112] axes of the inclusions and those of the diamonds is
117 remarkably small ($< 2^\circ$), i.e., within the uncertainty of the measurements (cf. Nestola et
118 al., 2014), and the inclusions appear to be mutually rotated around the [112] axis of their
119 host (Fig. 2).

120 The CL images of sample BZ270 show a complex growth–resorption pattern,
121 disturbed by plastic deformation (Fig. 1F–H), as commonly observed in sublithospheric
122 diamonds (Shirey et al., 2013). EBSD data are consistent with the activation of
123 $\{111\}\langle 011\rangle$ slip systems (Fig. DR3 in the GSA Data Repository¹), a mechanism
124 observed in several natural and experimentally deformed diamonds (Howell et al., 2012).
125 Domains characterized by slightly different lattice orientations (up to 3.5°) are observed,
126 which show no special relationship with the distribution of the inclusions (Fig. DR3).
127 Polishing of diamond BZ270 allowed us to uncover two of the FM inclusions and three
128 of the aligned, μm -sized inclusions. The FM inclusions sit on distinct diamond growth
129 zones (Fig. 1G). The analyzed μm -sized inclusions have a composition corresponding to
130 Ni-poor pyrrhotite (Table DR1), within the compositional range reported for other Juina
131 diamonds (Hutchison, 1997), and are located at the boundary between two more external
132 CL growth bands (Fig. 1H).

133 The compositions of the FM inclusions indicate an X_{Fe} range of ca. 0.33 to ≥ 0.64
134 (Table 1). Because high-quality XRD and EMPA data could be obtained only on some of
135 the inclusions, some X_{Fe} data have large uncertainties, but they are sufficient to establish
136 a relatively Fe-rich composition for all studied inclusions. Data for sample JUC4 suggest
137 a progressive X_{Fe} increase in inclusions sitting outside the N-rich diamond core. The
138 moderate NiO (0.4 wt. %) and very low Na₂O (< 0.06 wt. %) contents measured on

139 exposed inclusions n. 4 and 5 in diamond BZ270 (Table DR1) are in line with those
140 reported for FM inclusions of similar X_{Fe} in worldwide diamonds (Thomson et al., 2016).

141 **DISCUSSION AND CONCLUSIONS**

142 Data for multiple inclusions in two stones indicate a non-random COR between
143 FM and diamond (Fig. 2; Table DR2). The nearly parallel orientation of FM's and
144 diamond's crystal lattices suggests an original *specific COR* (cf. Griffiths et al., 2016).
145 Post-entrapment plastic deformation in the diamond along $\{111\}\langle 011\rangle$ slip systems (Fig.
146 DR3), with consequent slight rotation of the inclusions around the normal $[112]$ axis (Fig.
147 2), may well account for the small observed angular mismatch. Consistently, this
148 particular type of rotational COR was not observed in inclusions from less deformed
149 lithospheric diamonds (Nestola et al., 2014; Milani et al., 2016).

150 A specific COR may result from interface energy minimization (i) on
151 precipitation from a fluid/melt, during mutual growth or when one of the two minerals
152 provides a substrate for nucleation of the other (e.g., Mutaftschiev, 2001), (ii) on static
153 recrystallization, when the small effect of interface energies is not swamped in magnitude
154 by that of imposed stress (Wheeler et al., 2001), or (iii) on fluid/melt-assisted
155 recrystallization, when dissolution–precipitation and epitaxial nucleation of new grains
156 occur (Putnis and Austrheim, 2010). Scenario (ii) is highly unlikely in our case, given the
157 high-stress environment in which our diamonds have formed. Scenario (iii) is most likely
158 accompanied by chemical resetting and in fact, with increasing solid–fluid
159 disequilibrium, may grade into scenario (i). Note that the distinction between ‘fluid’ and
160 ‘melt’ tends to vanish with increasing pressure and may not exist under sub-lithospheric
161 conditions (Luth, 2014). Mechanical interactions between euhedral crystals can also

162 potentially lead to non-random COR (Wheeler et al., 2001). However, in this case only
163 one inclusion crystallographic direction, normal to the contact face, is fixed to the host.
164 Therefore, a statistical rotational relationship (cf. Griffiths et al., 2016) rather than a
165 strongly clustered orientation would be expected. Note that {112} faces are not found in
166 periclase-group minerals and are uncommon in diamond (Goldschmidt, 1916; Gaines et
167 al., 1997); therefore, they are unlikely to have played any role in determining the minor
168 rotational component in the observed COR (Fig. 2).

169 The distribution of the FM inclusions relative to diamond growth zones (Fig.
170 1G,H) and N zoning (Fig. 1D,E) indicates that at least some of them are sitting well away
171 from the diamond growth centers and, thus, cannot have acted as seeds for diamond
172 nucleation (cf. the ‘central inclusions’ in Bulanova, 1995, and Bulanova et al., 1998).
173 Moreover, none of the FM inclusions are located on healed cracks or subgrain boundaries
174 (Fig. 1G,H and DR3), which excludes that the inclusions were formed or modified after
175 diamond formation. Therefore, either diamond and FM precipitated from the same parent
176 medium, i.e., they are syngenetic, or FM nucleated epitaxially on diamond and was later
177 incorporated during a further episode of diamond growth. Whatever the nucleation
178 mechanism (dissolution–precipitation or precipitation as a new mineral), our Fe-rich FM
179 inclusions may not represent accidentally encapsulated portions of the ambient mantle,
180 but rather the product of reactions occurring during the growth history of diamond. A
181 similar conclusion can be drawn for the tiny pyrrhotite inclusions in diamond BZ270,
182 sitting at the boundary between two diamond growth zones (Fig. 1C,H). Their low-Cr,
183 low-Ni composition (Table DR1) suggests an ‘eclogitic’ or melt-rich environment.

184 FM compositions in diamond JUC4 ($X_{\text{Fe}} = 0.43$ to ≥ 0.64) show no overlap with
185 the range for FM in association with former bridgmanite ($X_{\text{Fe}} = 0.10$ – 0.36 , median =
186 0.17 , $N = 19$; Hutchison, 1997; Stachel et al., 2000; Davies et al., 2004; Hayman et al.,
187 2005; Tappert et al., 2009; Zedgenizov et al., 2014), and FM compositions in diamond
188 BZ270 are tightly clustered at its Fe-rich end. This suggests that the processes recorded in
189 our diamonds may not be typical of the lower mantle. Indeed, experiments by Thomson
190 et al. (2016) suggest that precipitation of variously Fe-enriched FM and diamond may
191 occur by reaction of slab-derived carbonatite melt with mantle rocks, at varying melt/rock
192 ratios, in the deep upper mantle and transition zone. This scenario is fully compatible
193 with our observations and provides a plausible mechanism for formation of our FM-
194 bearing diamonds at depths shallower than the lower mantle under increasing melt/rock
195 ratio.

196 Our interpretation of Fe-rich FM inclusions as a product of reactions occurring
197 during the growth history of diamond may potentially apply to other FM inclusions for
198 which evidence of pre-diamond formation is lacking. Therefore, using FM inclusions to
199 provide direct information on the composition of the ambient mantle and, particularly, of
200 the lower mantle is unwarranted. Specifically, a ‘non-pyrolitic’ composition of the lower
201 mantle is not required to explain the occurrence of Fe-rich FM inclusions in diamonds.
202 By identifying examples of mineral inclusions which reflect local growth conditions
203 rather than ambient mantle we emphasize the importance of, and provide a means for
204 testing host/inclusion time relationships in strongly deformed diamonds.

205 **ACKNOWLEDGMENTS**

206 Material for the present study was supplied by MTH. This research was supported
207 by the Alfred P. Sloan Foundation's Deep Carbon Observatory (DMGC-project), ERC
208 Starting Grant INDIMEDEA to FN (agreement n. 307322), CPDA 122324/12 and
209 FACCPRAT12 grants (University of Padova) and National Project PONa3_00369
210 "SISTEMA" (University of Bari). Constructive reviews by F. Kaminsky and two
211 anonymous reviewers helped us improve the manuscript.

212 REFERENCES CITED

- 213 Agrosi, G., Tempesta, G., Della Ventura, G., Cestelli Guidi, M., Hutchison, M., Nimis,
214 P., and Nestola, F., 2017, Non-destructive in situ study of plastic deformations in
215 diamonds: X-ray diffraction topography and μ FTIR mapping of two super deep
216 diamond crystals from São Luiz (Juina, Brazil): *Crystals*, v. 7, p. 233,
217 doi:<https://doi.org/10.3390/cryst7080233>.
- 218 Angel, R., Milani, S., Alvaro, M., and Nestola, F., 2015, OrientXplot: a program to
219 analyse and display relative crystal orientations: *Journal of Applied Crystallography*,
220 v. 48, p. 1330–1334, doi:<https://doi.org/10.1107/S160057671501167X>.
- 221 Bulanova, G.P., 1995, The formation of diamond: *Journal of Geochemical Exploration*,
222 v. 53, p. 1–23, [https://doi.org/10.1016/0375-6742\(94\)00016-5](https://doi.org/10.1016/0375-6742(94)00016-5).
- 223 Bulanova, G.P., Griffin, W.L., and Ryan, C.G., 1998, Nucleation environment of
224 diamonds from Yakutian kimberlites: *Mineralogical Magazine*, v. 62, p. 409–419,
225 doi:<https://doi.org/10.1180/002646198547675>.
- 226 Davies, R.M., Griffin, W.L., O'Reilly, S.Y., and Doyle, B.J., 2004, Mineral inclusions
227 and geochemical characteristics of microdiamonds from the DO27, A154, A21,

- 228 A418, DO18, DD17 and Ranch Lake kimberlites at Lac de Gras, Slave Craton,
229 Canada: *Lithos*, v. 77, p. 39–55, doi:<https://doi.org/10.1016/j.lithos.2004.04.016>.
- 230 Fei, Y., and Bertka, C.M., 1999, Phase transitions in the Earth's mantle and mantle
231 mineralogy, *in* Fei, Y., et al., eds., *Mantle Petrology: Field Observations and High*
232 *Pressure Experimentation; a Tribute to Francis R. (Joe) Boyd*: Geochemical Society
233 London Special Publication 6, p. 189–207.
- 234 Gaines, R.V., Catherine, H., Skinner, W., Foord, E.E., Mason, B., and Rosenzweig, A.,
235 1997, Dana's new mineralogy: the system of mineralogy of James Dwight Dana and
236 Edward Salisbury Dana, Eighth Edition: New York, John Wiley & Sons, Inc., 1819
237 p.
- 238 Goldschmidt, V., 1916, *Atlas der Krystallformen*: Heidelberg, Germany, Carl Winters
239 Universitatsbuchhandlung, 144 p.
- 240 Griffiths, T.A., Habler, G., and Abart, R., 2016, Crystallographic orientation relationships
241 in host–inclusion systems: New insights from large EBSD data sets: *The American*
242 *Mineralogist*, v. 101, p. 690–705, doi:<https://doi.org/10.2138/am-2016-5442>.
- 243 Harte, B., Harris, J.W., Hutchison, M.T., Watt, G.R., and Wilding, M.C., 1999, Lower
244 mantle mineral associations in diamonds from Sao Luiz, Brazil, *in* Fei, Y., et al.,
245 eds., *Mantle Petrology: Field Observations and High Pressure Experimentation; a*
246 *tribute to Francis R. (Joe) Boyd*: Geochemical Society, London, Special Publication
247 6, p. 125–153.
- 248 Harte, B., 2010, Diamond formation in the deep mantle: the record of mineral inclusions
249 and their distribution in relation to mantle dehydration zones: *Mineralogical*
250 *Magazine*, v. 74, p. 189–215, doi:<https://doi.org/10.1180/minmag.2010.074.2.189>.

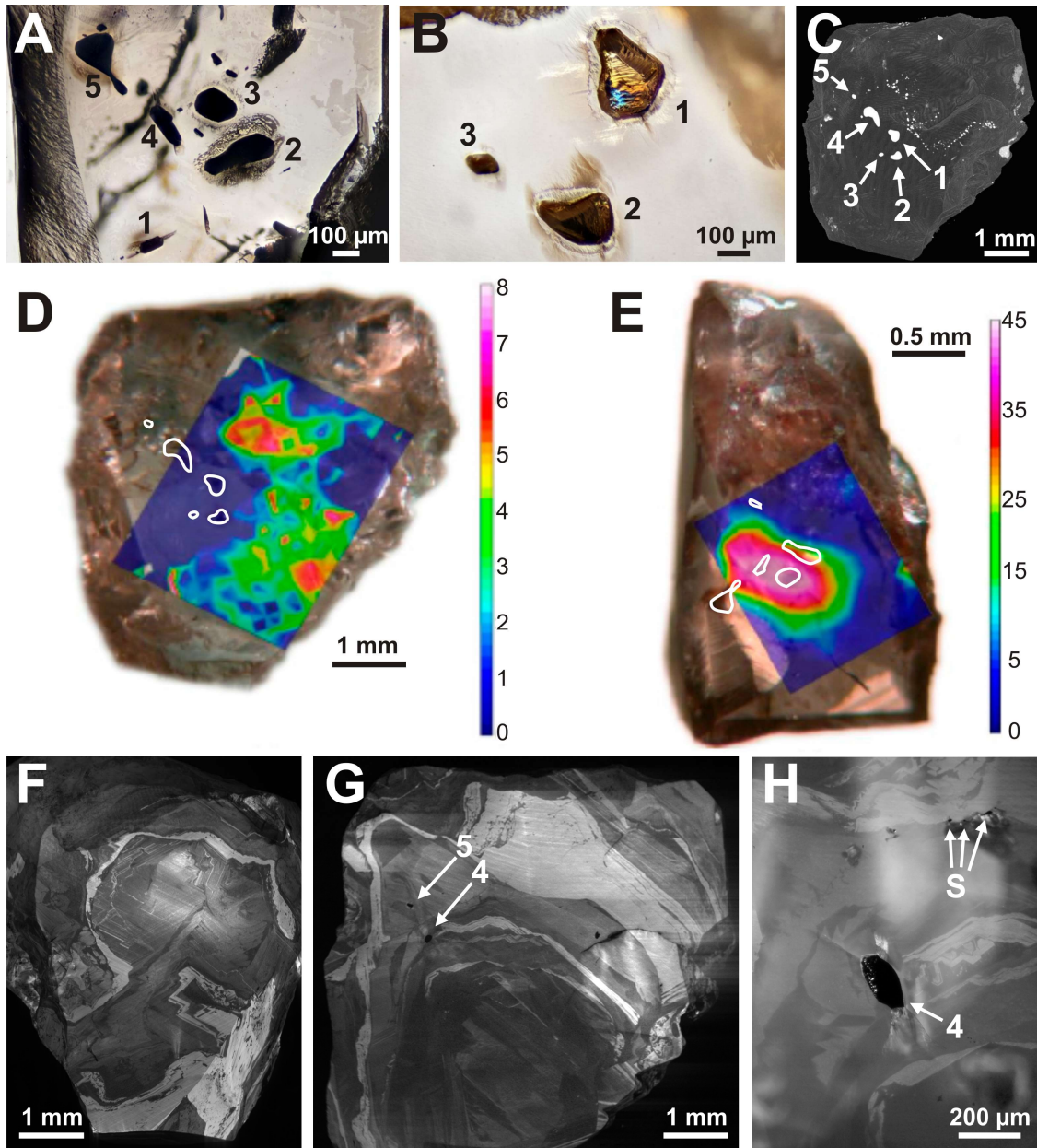
- 251 Hayman, P.C., Kopylova, M.G., and Kaminsky, F.V., 2005, Lower mantle diamonds
252 from Rio Soriso (Juina, Brazil): *Contributions to Mineralogy and Petrology*, v. 149,
253 p. 430–445, doi:<https://doi.org/10.1007/s00410-005-0657-8>.
- 254 Howell, D., Piazzolo, S., Dobson, D.P., Wood, I.G., Jones, A.P., Walte, N., Frost, D.J.,
255 Fisher, D., and Griffin, W.L., 2012, Quantitative characterization of plastic
256 deformation of single diamond crystals: A high pressure high temperature (HPHT)
257 experimental deformation study combined with electron backscatter diffraction
258 (EBSD): *Diamond and Related Materials*, v. 30, p. 20–30,
259 doi:<https://doi.org/10.1016/j.diamond.2012.09.003>.
- 260 Hutchison, M.T., 1997, Constitution of the deep transition zone and lower mantle shown
261 by diamonds and their inclusions [Ph.D. thesis]: University of Edinburgh, 660 p. and
262 CDRom.
- 263 Hutchison, M.T., Hursthouse, M.B., and Light, M.E., 2001, Mineral inclusions in
264 diamonds: associations and chemical distinctions around the 670-km discontinuity:
265 *Contributions to Mineralogy and Petrology*, v. 142, p. 119–126,
266 doi:<https://doi.org/10.1007/s004100100279>.
- 267 Hutchison, M.T., Nixon, P.H., and Harley, S.L., 2004, Corundum inclusions in diamonds
268 - discriminatory criteria and a corundum compositional database: *Lithos*, v. 77,
269 p. 273–286, doi:<https://doi.org/10.1016/j.lithos.2004.04.006>.
- 270 Irifune, T., 1994, Absence of an aluminous phase in the upper part of the Earth's lower
271 mantle: *Nature*, v. 370, p. 131–133, <https://doi.org/10.1038/370131a0>.

- 272 Kaminsky, F.V., 2012, Mineralogy of the lower mantle: A review of ‘super-deep’
273 mineral inclusions in diamond: *Earth-Science Reviews*, v. 110, p. 127–147,
274 doi:<https://doi.org/10.1016/j.earscirev.2011.10.005>.
- 275 Kaminsky, F.V., and Lin, J.-F., 2017, Iron partitioning in natural lower-mantle minerals:
276 Toward a chemically heterogeneous lower mantle: *The American Mineralogist*,
277 v. 102, p. 824–832, doi:<https://doi.org/10.2138/am-2017-5949>.
- 278 Kaminsky, F.V., Ryabchikov, I.D., McCammon, C.A., Longo, M., Abakumov, A.M.,
279 Turner, S., and Heidari, H., 2015, Oxidation potential in the Earth’s lower mantle as
280 recorded by ferropericlase inclusions in diamond: *Earth and Planetary Science*
281 *Letters*, v. 417, p. 49–56, doi:<https://doi.org/10.1016/j.epsl.2015.02.029>.
- 282 Kesson, S.E., and Fitz Gerald, J.D., 1992, Partitioning of MgO, FeO, NiO, MnO and
283 Cr₂O₃ between magnesian silicate perovskite and magnesiowüstite: implications for
284 the origin of inclusions in diamond and the composition of the lower mantle: *Earth*
285 *and Planetary Science Letters*, v. 111, p. 229–240, [https://doi.org/10.1016/0012-](https://doi.org/10.1016/0012-821X(92)90181-T)
286 [821X\(92\)90181-T](https://doi.org/10.1016/0012-821X(92)90181-T).
- 287 Lee, K.K.M., O’Neill, B., Panero, W.R., Shim, S.H., Benedetti, L.R., and Jeanloz, R.,
288 2004, Equations of state of the high-pressure phases of a natural peridotite and
289 implications for the Earth’s lower mantle: *Earth and Planetary Science Letters*,
290 v. 223, p. 381–393, doi:<https://doi.org/10.1016/j.epsl.2004.04.033>.
- 291 Litvin, Y.A., 2014, The stishovite paradox in the genesis of superdeep diamonds:
292 *Doklady Earth Sciences*, v. 455, p. 274–278,
293 doi:<https://doi.org/10.1134/S10283334X14030064>.

- 294 Liu, L., 2002, An alternative interpretation of lower mantle mineral associations in
295 diamonds: *Contributions to Mineralogy and Petrology*, v. 144, p. 16–21,
296 doi:<https://doi.org/10.1007/s00410-002-0389-y>.
- 297 Luth, R.W., 2014, 3.9 — Volatiles in Earth's mantle, *in* Holland, H.D., and Turekian,
298 K.K., eds., *Treatise on Geochemistry*: Elsevier Oxford, p. 355–391, doi:
299 <https://doi.org/10.1016/B978-0-08-095975-7.00207-2>.
- 300 Milani, S., Nestola, F., Angel, R.J., Nimis, P., and Harris, J.W., 2016, Crystallographic
301 orientations of olivine inclusions in diamonds: *Lithos*, v. 265, p. 312–316,
302 <https://doi.org/10.1016/j.lithos.2016.06.010>.
- 303 Mutaftschiev, B., 2001, *The Atomistic Nature of Crystal Growth*: Springer-Verlag Berlin
304 Heidelberg New York, v. 43, 368 p.
- 305 Nestola, F., Nimis, P., Angel, R.J., Milani, S., Bruno, M., Prencipe, M., and Harris, J.W.,
306 2014, Olivine with diamond-imposed morphology included in diamonds. Syngensis
307 or protogenesis?: *International Geology Review*, v. 56, p. 1658–1667,
308 doi:<https://doi.org/10.1080/00206814.2014.956153>.
- 309 Otsuka, K., Longo, M., McCammon, C.A., and Karato, S.-i., 2013, Ferric iron content of
310 ferropericlase as a function of composition, oxygen fugacity, temperature and
311 pressure: implications for redox conditions during diamond formation in the lower
312 mantle: *Earth and Planetary Science Letters*, v. 365, p. 7–16,
313 <https://doi.org/10.1016/j.epsl.2012.11.030>.
- 314 Putnis, A., and Austrheim, H., 2010, Fluid-induced processes: Metasomatism and
315 metamorphism: *Geofluids*, v. 10, p. 254–269, doi:10.1111/j.1468-
316 8123.2010.00285.x.

- 317 Ryabchikov, I.D., and Kaminsky, F.V., 2013, The composition of the lower mantle:
318 Evidence from mineral inclusions in diamonds: *Doklady Earth Sciences*, v. 453,
319 p. 1246–1249, <https://doi.org/10.1134/S1028334X13120155>.
- 320 Shirey, S.B., Cartigny, P., Frost, D.J., Keshav, S., Nestola, F., Nimis, P., Pearson, D.G.,
321 Sobolev, N.V., and Walter, M.J., 2013, Diamonds and the geology of mantle carbon,
322 *in* Hazen, R.M., et al., eds., *Carbon in Earth: Reviews in Mineralogy and*
323 *Geochemistry*, v. 75, p. 355–421, doi:<https://doi.org/10.2138/rmg.2013.75.12>.
- 324 Stachel, T., Brey, G.P., and Harris, J.W., 2005, Inclusions in sublithospheric diamonds:
325 glimpses of deep Earth: *Elements*, v. 1, p. 73–78,
326 doi:<https://doi.org/10.2113/gselements.1.2.73>.
- 327 Stachel, T., Harris, J.W., Brey, G.P., and Joswig, W., 2000, Kankan diamonds (Guinea)
328 II: lower mantle inclusion paragenesis: *Contributions to Mineralogy and Petrology*,
329 v. 140, p. 16–27, <https://doi.org/10.1007/s004100000174>.
- 330 Tappert, R., Foden, J., Stachel, T., Muehlenbachs, K., Tappert, M., and Wills, K., 2009,
331 Deep mantle diamonds from South Australia: A record of Pacific subduction at the
332 Gondwanan margin: *Geology*, v. 37, p. 43–46,
333 doi:<https://doi.org/10.1130/G25055A.1>.
- 334 Thomson, A.R., Kohn, S.C., Bulanova, G.P., Smith, C.B., Araujo, D., EIMF, and Walter,
335 M.J., 2014, Origin of sub-lithospheric diamonds from the Juina-5 kimberlite (Brazil):
336 constraints from carbon isotopes and inclusion compositions: *Contributions to*
337 *Mineralogy and Petrology*, v. 168, p. 1081, doi:[https://doi.org/10.1007/s00410-014-](https://doi.org/10.1007/s00410-014-1081-8)
338 1081-8.

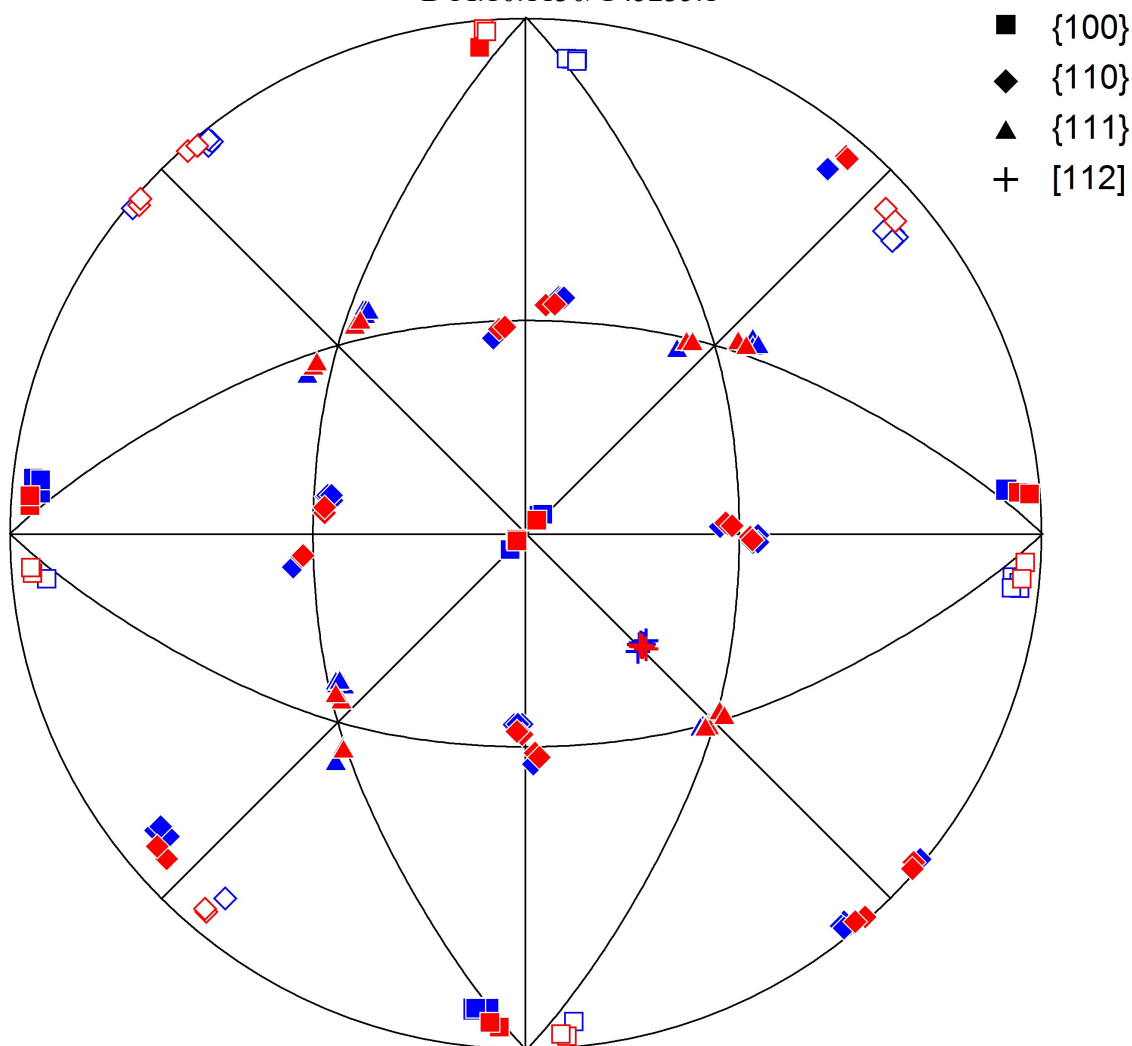
- 339 Thomson, A.R., Walter, M.J., Kohn, S.C., and Brooker, R.A., 2016, Slab melting as a
340 barrier to deep carbon subduction: *Nature*, v. 529, p. 76–79,
341 doi:<https://doi.org/10.1038/nature16174>.
- 342 Wheeler, J., Prior, D.J., Jiang, Z., Spiess, R., and Trimby, P.J., 2001, The petrological
343 significance of misorientations between grains: *Contributions to Mineralogy and
344 Petrology*, v. 141, p. 109–124, <https://doi.org/10.1007/s004100000225>.
- 345 Wood, B.J., 2000, Phase transformations and partitioning relations in peridotite under
346 lower mantle conditions: *Earth and Planetary Science Letters*, v. 174, p. 341–354,
347 doi:[https://doi.org/10.1016/S0012-821X\(99\)00273-3](https://doi.org/10.1016/S0012-821X(99)00273-3).
- 348 Zedgenizov, D.A., Kagi, H., Shatsky, V.S., and Ragozin, A.L., 2014, Local variations of
349 carbon isotope composition in diamonds from São-Luis (Brazil): evidence for
350 heterogeneous carbon reservoir in sublithospheric mantle: *Chemical Geology*,
351 v. 363, p. 114–124, <https://doi.org/10.1016/j.chemgeo.2013.10.033>.
- 352
- 353



354

355 Figure 1. (A-B) Microphotographs of FM inclusions in polished diamonds JUC4 (A,
356 transmitted light) and BZ270 (B, transmitted plus incident light); (C) μ -CT image of
357 diamond BZ270, showing a cluster of FM inclusions (numbered) and a trail of tiny
358 inclusions; (D) FTIR map of diamond BZ270; the color scale, from blue (zero intensity)
359 to red/whitish (max intensity), is qualitative and given the low values is not necessarily

360 related to N concentration; white outlines indicate projection of the FM inclusions (mod.
361 after Agrosi et al., 2017); (E) same as in (D) for diamond JUc4, but here the color scale
362 has been confirmed to correlate to N concentration (mod. after Agrosi et al., 2017); (F)
363 CL image of diamond BZ270 after limited polishing; (G-H) CL images of reverse side of
364 diamond BZ270 after different degrees of polishing, with exposed FM and sulfide (S)
365 inclusions. Numbers in (A-C) and (G-H) as in Table 1.
366
367



368

369 Figure 2. Crystallographic orientations of FM inclusions relative to their diamond hosts,
370 plotted using the OrientXplot software (Angel et al., 2015). Open symbols plot in lower
371 hemisphere. Blue symbols = BZ270; red symbols = JUc4.

372

373 1GSA Data Repository item 2018xxx, sample location and analytical methods and micro-
374 computed X-ray tomography (μ -CT) of diamond BZ270 (video), is available online at
375 <http://www.geosociety.org/datarepository/2018/>, or on request from
376 editing@geosociety.org.

377
 378
 379
 380
 381
 382
 383
 384
 385
 386
 387
 388

TABLE 1. COMPOSITIONAL DATA FOR FM INCLUSIONS

Diamond	Inclusion	X_{Fe} (site occ.) [*]	X_{Fe} (a edge) [†]	X_{Fe} (EMPA) [§]
BZ270	1	0.31(2)	≥0.34(2)	–
	2	0.31(2)	≥0.35(2)	–
	3	–	≥0.35(5)	–
	4	–	0.34(2)	0.346(3)
	5	0.36(2)	0.35(2)	0.338(0)
JUc4	2	–	≥0.57(5)	–
	3	–	≥0.44(5)	–
	4	–	≥0.43(6)	–
	5	–	≥0.64(3)	–

Note: Numbers in parentheses are 1·σ uncertainties on the last digit. See the Data Repository¹ for details on evaluation of chemical compositions.

^{*}Based on site occupancies after crystal structure refinement.

[†]Based on equation $X_{Fe} = 8.441 \cdot a (\text{Å}) - 35.553$, valid for stoichiometric FM at room pressure; minimum values for unexposed inclusions analyzed in situ, which may be under residual pressure.

[§]Based on EMPA analysis of exposed inclusions (Table DR1).

389
 390